POLITECNICO DI TORINO
Repository ISTITUZIONALE

ENERGY-EFFICIENT MIMO COMMUNICATION ASSISTED BY METASURFACES WITH GLOBAL REFLECTION

Original
ENERGY-EFFICIENT MIMO COMMUNICATION ASSISTED BY METASURFACES WITH GLOBAL REFLECTION CONSTRAINTS / Tunal, I., Kuku Fotock, R., Zappone, A., Taricco, G., Ali Cirpan, H.. - (2025), pp. 131-136. (International Conference on Electromagnetics in Advanced Applications 2025 Palermo (Ita) 8-12 September 2025).

Availability:
This version is available at: 11583/3002895 since: 2025-09-13T20:19:31Z

Publisher:
IEEE

Published
DOI:

Terms of use:

This article is made available under terms and conditions as specified in the corresponding bibliographic description in the repository

Publisher copyright
IEEE postprint/Author's Accepted Manuscript

©2025 IEEE. Personal use of this material is permitted. Permission from IEEE must be obtained for all other uses, in any current or future media, including reprinting/republishing this material for advertising or promotional purposes, creating new collecting works, for resale or lists, or reuse of any copyrighted component of this work in other works.

(Article begins on next page)

25 November 2026

Energy-Efficient MIMO Communication Assisted by Metasurfaces with Global Reflection Constraints

Ayşegul Ilay Tunali [*†§] Robert Kuku Fotock [‡] Alessio Zappone [‡*]

Giorgio Taricco [†] Hakan Ali Çırpan [§]

[*] Consorzio Nazionale Interuniversitario per le Telecomunicazioni - CNIT, Italy
[†] Politecnico di Torino, Italy
[‡] University of Cassino and Southern Lazio, Italy
[§] Istanbul Technical University, Turkey

***Abstract*—This paper investigates the design of a MIMO communication system enhanced by a reconfigurable holographic surface (RHS) positioned near the transmitter. The system is optimized through the joint design of the transmit covariance matrix and the RHS reflection coefficients. The RHS is configured using sequential fractional programming, while two strategies are explored for optimizing the transmit covariance matrix: one based on fractional programming, and the other involving a search over a standard-compliant codebook. A performance comparison between the two methods demonstrates that the codebook-based approach achieves results close to those of the more computationally intensive fractional programming method. Both passive and active RHS implementations—where the latter includes analog amplification—are considered, providing a comprehensive analysis of system performance under varying hardware capabilities.**

***Index Terms*—Holographic beamforming, reconfigurable holographic metasurfaces, reconfigurable intelligent surfaces, energy efficiency, radio resource allocation.**

I. Introduction

ENHANCING the Energy Efficiency (EE) is essential for the development of future 6G wireless networks, as existing systems that utilize active antennas demand significant energy, which is increasingly unsustainable in light of the rising demand for mobile connectivity and the introduction of new services. With EE as a key objective, metasurfaces offer a promising solution—particularly in massive Multiple-Input Multiple-Output (MIMO) communication scenarios—by enabling a reduction in the number of antennas needed at both the transmitter and receiver, while still maintaining array gain due to the high density of surface elements. Existing literature on metasurface-assisted communication systems primarily concentrates on scenarios involving Base Stations (BSs) with multiple antennas and mobile terminals with a single antenna, mainly because this setup offers greater analytical simplicity (see, e.g. [1]–[3]). These systems provide array gain but lack multiplexing gain, which significantly limits both the achievable data rate and energy efficiency. Furthermore, most prior studies on EE optimization assume that the metasurfaces are positioned in the far-field region of the transmitting array. Among the few studies focused on EE optimization in metasurface-aided MIMO systems, [4] provides upper and lower bounds on the EE of a single-stream transmission MIMO link, while [5] investigates the trade-off between EE and spectral efficiency, employing the weighted minimum mean squared error method to tackle the problem. In [6], for a MIMO link employing Simultaneous Information and Power Transfer (SWIPT), the problem of minimizing the difference between rate and power is addressed, with the aim of improving the EE of the link. Finally, in [7], a MIMO network with finite block-length transmissions is considered, and the network EE is optimized through sequential fractional programming. The main contribution of this work can be summarized as follows:

- We address the problem of maximizing the EE in a MIMO link using holographic beamforming through a metasurface. In our scenario, both the transmitter and receiver are equipped with multiple antennas, and the metasurface is positioned close to the transmitter. Here, we refer to the metasurface as a Reconfigurable Holographic Surface (RHS). The proposed model incorporates both far-field and near-field signal propagation, allowing for the deployment of the metasurface within the near-field of the base station antennas.
- In the proposed setup, we introduce a new, provably convergent, optimization algorithm to maximize the EE, built on a novel reformulation of rank-one constraints combined with sequential programming. Unlike existing optimization methods for metasurface-aided MIMO systems that work with matrix-valued functions, our approach optimizes a vector-valued function sequentially. As a result, the complexity of our algorithm is significantly reduced.
- The optimization of the transmit covariance matrix is approached by conducting a search within standard-compliant codebooks.
- In this work, we focus on metasurfaces with global reflection constraints, which are more general than the traditional metasurfaces with local reflection constraints. Specifically, while the latter focus on each reflecting element individually, ensuring that the modulus of each local reflection coefficient does not exceed one, the

former focus on ensuring that the total power reflected by the entire metasurface does not exceed the total power incident on it.

II. System model and problem formulation

We focus on a single-user MIMO link, where an N_T-antenna equipped BS communicates with a mobile terminal with N_R antennas, through a nearly-passive RHS, equipped with N reflecting elements. Both transmit and receive antenna arrays, and RHS elements, are arranged in a rectangular pattern, with horizontal and vertical spacing given by $(\Delta_{h,t}, \Delta_{v,t})$ for the transmit antenna array, by $(\Delta_{h,r}, \Delta_{v,r})$ for the receive antenna array, and by (Δ_h, Δ_v) for the RHS. The RHS is deployed in the proximity of the transmit antennas, namely in the near-field zone of the transmit antenna array.

A. Channel model

Let $\boldsymbol{H}$ and $\boldsymbol{G}$ be the $N \times N_T$ and $N_R \times N$ channel matrices corresponding to the links between the BS and the RHS and between the RHS and the receiver, respectively. Since the RHS is in the near-field of the transmit array, the entries of the BS to RHS channel matrix can be written exploiting the spherical wave equation, i.e. the (n,m) element of $\boldsymbol{H}$, with $n = 1, \ldots, N$ and $m = 1, \ldots, N_T$, is expressed as

$$H(n,m) = \frac{\lambda}{4\pi}\sqrt{\alpha^{RHS}_{n,m}\alpha^{BS}_{n,m}}\frac{e^{-\left[j(2\pi/\lambda)\|\boldsymbol{r}^{RHS}_n - \boldsymbol{r}^{BS}_m\|\right]}}{\|\boldsymbol{r}^{RHS}_n - \boldsymbol{r}^{BS}_m\|} \ . \quad (1)$$

Here, the vectors $\boldsymbol{r}^{RHS}_n$ and $\boldsymbol{r}^{BS}_m$ represent the positions of the n-th RHS element and m-th BS antenna, $\alpha^{BS}_{m,n}$ denotes the transmit gain of the m-th transmit antenna towards the n-th RHS element and $\alpha^{RHS}_{m,n}$ denotes the receive gain of the n-th RHS element from the m-th transmit antenna, expressed by:

$$\alpha^{BS}_{n,m} = \frac{4\pi}{\lambda^2}\Delta_{h,t}\Delta_{v,t}\rho^{BS}_{n,m} \quad (2)$$

$$\alpha^{RHS}_{n,m} = \frac{4\pi}{\lambda^2}\Delta_h\Delta_v\rho^{RHS}_{n,m} \ , \quad (3)$$

with $\rho^{BS}_{n,m}$ and $\rho^{RHS}_{n,m}$ the standard directivity factors of the BS antenna array and RHS, respectively [8], [9].

A traditional far field model holds, instead, for the channel between the RHS and the receiver; therefore, we consider that each entry of $\boldsymbol{G}$ is a realization of a Rice random variable with factor K, scaled by the path-loss coefficient

$$\text{PL} = \text{PL}_0\left(\frac{d}{d_0}\right)^{-\nu} \ , \quad (4)$$

with PL_0 the path-loss at the reference distance d_0, d the RHS-receiver distance, and ν the path-loss exponent.

Additionally, we denote by $\boldsymbol{Q}$ the transmit covariance matrix, by $\boldsymbol{\Gamma} = \text{diag}(\gamma_{1,1}, \ldots, \gamma_{N,N})$ the RHS matrix, by $\boldsymbol{s}$ the $N_T \times 1$ vector of transmit symbols, with $\mathbb{E}[\boldsymbol{s}\boldsymbol{s}^H] = \boldsymbol{I}_{N_T}$, by $\boldsymbol{n} \sim \mathcal{CN}(\boldsymbol{0}, \sigma^2\boldsymbol{I})$ the thermal noise at the receiver, and, finally, by B the communication bandwidth. Then, the signal impinging on the RHS can be expressed as

$$\boldsymbol{y} = \boldsymbol{H}\boldsymbol{Q}^{1/2}\boldsymbol{s} \ , \quad (5)$$

and, in turn, the signal received at the final destination, reflected on the RHS represented by $\boldsymbol{\Gamma}$, and propagating over the channel $\boldsymbol{G}$, can be written as

$$\boldsymbol{y} = \boldsymbol{G}\boldsymbol{\Gamma}\boldsymbol{H}\boldsymbol{Q}^{1/2}\boldsymbol{s} + \boldsymbol{n} \quad (6)$$

(notice that the metasurface does not introduce noise amplification, being a passive device). The total hardware power consumed in the system, say P_c, is given by

$$P_c = NP_{c,n} + N_TP_{c,t} + N_RP_{c,r} + P_{c,0} \ , \quad (7)$$

where $P_{c,n}$ is the static power used by each metasurface element, $P_{c,t}$ is the static power used by each antenna of the transmit array, $P_{c,r}$ is the static power used by each antenna of the receive array, and $P_{c,0}$ is the static power used by all other circuitry in the system. Then, denoting by $\mu \geq 1$ the inverse of the transmit amplifier efficiency, the total power consumption of the system amounts to $P_t = \mu\text{tr}(\boldsymbol{Q}) + P_c$, and the system capacity and EE are given by

$$C = B\log_2\det\left(\boldsymbol{I} + \frac{1}{\sigma^2}\boldsymbol{G}\boldsymbol{\Gamma}\boldsymbol{H}\boldsymbol{Q}\boldsymbol{H}^H\boldsymbol{\Gamma}^H\boldsymbol{G}^H\right) \ , \text{ [bit/s]} \quad (8)$$

$$\text{EE} = \frac{C}{P_t} = B\frac{\log_2\det\left(\boldsymbol{I} + \frac{1}{\sigma^2}\boldsymbol{G}\boldsymbol{\Gamma}\boldsymbol{H}\boldsymbol{Q}\boldsymbol{H}^H\boldsymbol{\Gamma}^H\boldsymbol{G}^H\right)}{\mu\text{tr}(\boldsymbol{Q}) + P_c} \ , \text{ [bit/J]} \quad (9)$$

In this work, we consider a metasurface with global reflection constraints, i.e. the reflection matrix $\boldsymbol{\Gamma}$ is required to satisfy $P_{out} \leq P_{in}$, where P_{out} is the power that departs from the metasurface and P_{in} is the power that impinges on the metasurface. These powers are given by

$$P_{in} = \mathbb{E}[\text{tr}(\boldsymbol{H}\boldsymbol{Q}^{1/2}\boldsymbol{s}\boldsymbol{s}^H\boldsymbol{Q}^{1/2}\boldsymbol{H}^H)] = \text{tr}(\boldsymbol{H}\boldsymbol{Q}\boldsymbol{H}^H) \quad (10)$$

$$P_{out} = \mathbb{E}[\text{tr}(\boldsymbol{\Gamma}\boldsymbol{H}\boldsymbol{Q}^{1/2}\boldsymbol{s})(\boldsymbol{s}^H\boldsymbol{Q}^{1/2}\boldsymbol{H}^H\boldsymbol{\Gamma}^H)] = \text{tr}(\boldsymbol{\Gamma}\boldsymbol{H}\boldsymbol{Q}\boldsymbol{H}^H\boldsymbol{\Gamma}^H) \quad (11)$$

Thus, the global reflection constraint at the metasurface is expressed by:

$$\text{tr}(\boldsymbol{\Gamma}\boldsymbol{H}\boldsymbol{Q}\boldsymbol{H}^H\boldsymbol{\Gamma}^H) \leq \text{tr}(\boldsymbol{H}\boldsymbol{Q}\boldsymbol{H}^H) \ . \quad (12)$$

Moreover, denoting by P_{max} the maximum transmit power at the BS, the problem of EE maximization with respect to the metasurface matrix and the transmit covariance matrix can be cast as

$$\max_{\boldsymbol{Q},\boldsymbol{\Gamma}} B\frac{\log_2\left|\boldsymbol{I} + \frac{1}{\sigma^2}\boldsymbol{G}\boldsymbol{\Gamma}\boldsymbol{H}\boldsymbol{Q}\boldsymbol{H}^H\boldsymbol{\Gamma}^H\boldsymbol{G}^H\right|}{\mu\text{tr}(\boldsymbol{Q}) + P_c} \quad (13a)$$

$$\text{s.t. } \text{tr}(\boldsymbol{\Gamma}\boldsymbol{H}\boldsymbol{Q}\boldsymbol{H}^H\boldsymbol{\Gamma}^H) \leq \text{tr}(\boldsymbol{H}\boldsymbol{Q}\boldsymbol{H}^H) \quad (13b)$$

$$\text{tr}(\boldsymbol{Q}) \leq P_{max} \ , \ \boldsymbol{Q} \succeq \boldsymbol{0} \quad (13c)$$

Problem (13) is a non-convex fractional program, which cannot be solved by basic convex optimization or fractional programming theory, due to the fact that, with respect to $(\boldsymbol{Q}, \boldsymbol{\Gamma})$: $i)$ the numerator of (13a) is not concave and $ii)$ the constraint (13b) is not convex. To solve problem (13) we resort to a reformulation of the RHS optimization problem, and optimize the covariance matrix $\boldsymbol{Q}$ by a search in finite

set, which is a standard-compliant codebook. Perfect channel state information (CSI) is assumed to be available for resource allocation purposes. This assumption applies to a situation in which both the transmitter and the receiver are static or moving at low velocity (e.g., the case of a channel between a BS and a pedestrian user), which leads to a channel coherence time that contains a large number of symbol intervals. In this scenario, traditional channel estimation techniques can be employed to to track $\boldsymbol{G}$, while, as previously discussed, the channel matrix $\boldsymbol{H}$, is perfectly known.

The proposed approach to solve problem (13) leverages on the alternating optimization framework by treating separately the optimization of the reflection matrix $\boldsymbol{\Gamma}$ and of the transmit covariance matrix $\boldsymbol{Q}$. The optimization of the metasurface will be treated in Section III, while the optimization of the transmit covariance matrix will be discussed in Section IV.

III. RHS Optimization for EE Maximization

Since the denominator of the EE does not depend on $\boldsymbol{\Gamma}$, the optimization of $\boldsymbol{\Gamma}$, for fixed $\boldsymbol{Q}$, reduces to the maximization of the system capacity, namely

$$\max_{\boldsymbol{\Gamma}} \log_2 \left| \boldsymbol{I} + \frac{1}{\sigma^2} \boldsymbol{G}\boldsymbol{\Gamma}\boldsymbol{A}\boldsymbol{\Gamma}^H\boldsymbol{G}^H \right| \tag{14a}$$

$$\text{s.t. } \mathrm{tr}(\boldsymbol{\Gamma}\boldsymbol{A}\boldsymbol{\Gamma}^H) \leq \mathrm{tr}(\boldsymbol{A}), \tag{14b}$$

where we defined $\boldsymbol{A} \triangleq \boldsymbol{H}\boldsymbol{Q}\boldsymbol{H}^H$. Problem (14) is non-convex, due to the non-concavity of[1] (14a). In order to address this, we express the matrix $\boldsymbol{A}$ by its eigenvalue decomposition, namely

$$\boldsymbol{A} = \sum_{\ell=1}^{N} \lambda_\ell \boldsymbol{u}_\ell \boldsymbol{u}_\ell^H \ , \tag{15}$$

with λ_ℓ and $\boldsymbol{u}_\ell$ the ℓ-th eigenvalue and eigenvector of $\boldsymbol{H}\boldsymbol{Q}\boldsymbol{H}^H$. Then,

$$\begin{aligned} \boldsymbol{\Gamma}\boldsymbol{A}\boldsymbol{\Gamma}^H &= \boldsymbol{\Gamma}\left(\sum_{\ell=1}^{N} \lambda_\ell \boldsymbol{u}_\ell \boldsymbol{u}_\ell^H\right)\boldsymbol{\Gamma}^H = \left(\sum_{\ell=1}^{N} \lambda_\ell \boldsymbol{\Gamma}\boldsymbol{u}_\ell \boldsymbol{u}_\ell^H \boldsymbol{\Gamma}^H\right) \\ &= \left(\sum_{\ell=1}^{N} \lambda_\ell \boldsymbol{U}_\ell \boldsymbol{\gamma}\boldsymbol{\gamma}^H \boldsymbol{U}_\ell^H\right) \ . \end{aligned} \tag{16}$$

Here, $\boldsymbol{U}_\ell = \mathrm{diag}(\boldsymbol{u}_\ell)$, $\boldsymbol{\gamma} = [\gamma_{1,1}, \ldots, \gamma_{N,N}]^T$, and we used the fact that $\boldsymbol{\Gamma}\boldsymbol{u}_\ell = \mathrm{diag}(\boldsymbol{u}_\ell)\boldsymbol{\gamma} = \boldsymbol{U}_\ell\boldsymbol{\gamma}$. As a result, Problem (14) can be restated as follows:

$$\max_{\boldsymbol{\gamma}} \log_2 \left| \boldsymbol{I} + \frac{1}{\sigma^2} \boldsymbol{G}\left(\sum_{\ell=1}^{N} \lambda_\ell \boldsymbol{U}_\ell \boldsymbol{\gamma}\boldsymbol{\gamma}^H \boldsymbol{U}_\ell^H\right)\boldsymbol{G}^H \right| \tag{17a}$$

$$\text{s.t. } \sum_{\ell=1}^{N} \lambda_\ell \mathrm{tr}\left(\boldsymbol{U}_\ell \boldsymbol{\gamma}\boldsymbol{\gamma}^H \boldsymbol{U}_\ell^H\right) \leq \mathrm{tr}(\boldsymbol{A}) \ . \tag{17b}$$

Problem (17) is still unsolvable because the objective function is not concave with respect to $\boldsymbol{\gamma}$. However, it is concave with respect to $\boldsymbol{\gamma}\boldsymbol{\gamma}^H$, which suggests to resort to the method of *semidefinite relaxation*. However, this approach has the disadvantage of potentially requiring a rank reduction step, which could impair performance and provides no guarantee regarding the efficiency of the optimized matrix $\boldsymbol{\Gamma}$. Therefore, we resort to a different approach.

We still introduce the new variable $\boldsymbol{R} = \boldsymbol{\gamma}\boldsymbol{\gamma}^H$, but, unlike the previous method, we do not relax the rank-one constraint on $\boldsymbol{R}$ but we reformulate it in a more tractable way. Namely, defining $\boldsymbol{R} = \boldsymbol{\gamma}\boldsymbol{\gamma}^H$, leads to the following problem:

$$\max_{\boldsymbol{R}\succeq\boldsymbol{0},\boldsymbol{\gamma}} \log_2 \left| \boldsymbol{I} + \frac{1}{\sigma^2} \boldsymbol{G}\left(\sum_{\ell=1}^{N} \lambda_\ell \boldsymbol{U}_\ell \boldsymbol{R} \boldsymbol{U}_\ell^H\right)\boldsymbol{G}^H \right| \tag{18a}$$

$$\text{s.t. } \sum_{\ell=1}^{N} \lambda_\ell \mathrm{tr}\left(\boldsymbol{U}_\ell \boldsymbol{R} \boldsymbol{U}_\ell^H\right) \leq \mathrm{tr}(\boldsymbol{A}) \tag{18b}$$

$$\mathrm{rank}(\boldsymbol{R}) = 1 \tag{18c}$$

Then, we resort to the following proposition, whose proof is contained in the extended journal version of this work, see [10], for space limitation.

Proposition 1. *Consider the following optimization problem.*

$$\max_{\boldsymbol{R}\succeq\boldsymbol{0},\boldsymbol{\gamma}} \log_2 \left| \boldsymbol{I} + \frac{1}{\sigma^2} \boldsymbol{G}\left(\sum_{\ell=1}^{N} \lambda_\ell \boldsymbol{U}_\ell \boldsymbol{R} \boldsymbol{U}_\ell^H\right)\boldsymbol{G}^H \right| \tag{19a}$$

$$\textit{s.t. } \sum_{\ell=1}^{N} \lambda_\ell \mathrm{tr}\left(\boldsymbol{U}_\ell \boldsymbol{R} \boldsymbol{U}_\ell^H\right) \leq \mathrm{tr}(\boldsymbol{A}) \tag{19b}$$

$$\begin{bmatrix} \boldsymbol{R} & \boldsymbol{\gamma} \\ \boldsymbol{\gamma}^H & 1 \end{bmatrix} \succeq \boldsymbol{0} \tag{19c}$$

$$\mathrm{tr}(\boldsymbol{R}) \leq \|\boldsymbol{\gamma}\|^2 \tag{19d}$$

Then, any $\boldsymbol{R}$ that is feasible for Problem (19)*, has rank equal to* 1 *and so is feasible for Problem* (18)*, too.*

Despite the application of Proposition 1, Problem (19) is still non-convex, due to the non-convexity of constraint (19d). However, this problem is more tractable than Problem (18), because the function in the non-convex constraint (19d) are differentiable, while the rank function in (18) is not. This allows us to resort to the sequential programming framework [2] to develop an iterative algorithm that monotonically improves the objective value of Problem (19), eventually converging to a first-order optimal point of (19). To this purpose, we notice that

$$\|\boldsymbol{\gamma} - \bar{\boldsymbol{\gamma}}\|^2 \geq 0 \implies \|\boldsymbol{\gamma}\|^2 \geq 2\Re\{\bar{\boldsymbol{\gamma}}^H\boldsymbol{\gamma}\} - \|\bar{\boldsymbol{\gamma}}\|^2. \tag{20}$$

This allows to replace Problem (19) by Problem (21), which satisfies the sequential optimization framework requirements[3]. Finally, the sequential optimization Algorithm 1 yields a first-order optimal solution of Problem (19), while monotonically

[1] Indeed, in the special case of a single-antenna system and a metasurface with only one reflecting element γ, (14) would reduce to $\log_2(1+g^2a^2|\gamma|^2)$, with ga the equivalent SISO channel gain. Clearly, not even in this simplified special case (14) is concave in γ.

[2] The fundamentals of sequential programming can be found in [11].

[3] Notice that inequality (21d) implies (19d), according to the requirements of the sequential method.

increasing the objective function after each iteration. Problem (21) is expressed as follows:

$$\max_{\boldsymbol{R}\succeq\mathbf{0},\boldsymbol{\gamma}} \log_2 \left| \boldsymbol{I} + \frac{1}{\sigma^2}\boldsymbol{G}\left(\sum_{\ell=1}^{N}\lambda_\ell \boldsymbol{U}_\ell \boldsymbol{R}\boldsymbol{U}_\ell^H\right)\boldsymbol{G}^H \right| \tag{21a}$$

$$\text{s.t.} \sum_{\ell=1}^{N}\lambda_\ell \mathrm{tr}\left(\boldsymbol{U}_\ell \boldsymbol{R}\boldsymbol{U}_\ell^H\right) \le \mathrm{tr}(\boldsymbol{H}\boldsymbol{Q}\boldsymbol{H}^H) \tag{21b}$$

$$\begin{bmatrix} \boldsymbol{R} & \boldsymbol{\gamma} \\ \boldsymbol{\gamma}^H & 1 \end{bmatrix} \succeq \mathbf{0} \tag{21c}$$

$$\mathrm{tr}(\boldsymbol{R}) - 2\Re\{\bar{\boldsymbol{\gamma}}^H\boldsymbol{\gamma}\} + \|\bar{\boldsymbol{\gamma}}\|^2 \le 0\,, \tag{21d}$$

Algorithm 1 RHS optimization

```
Choose ε > 0;
Set γ̄ to a feasible value;
repeat
    Solve (21) and denote its solution by (R*, γ*);
    Err = |γ* − γ̄|;
    γ̄ = γ*;
until Err ≤ ε
```

IV. Transmit covariance optimization

This section addresses the optimization of the covariance matrix $\boldsymbol{Q}$ according to two different approaches.

A. Optimization by fractional programming

The optimization with respect to $\boldsymbol{Q}$, for fixed $\boldsymbol{\Gamma}$, can be stated as follows:

$$\max_{\boldsymbol{Q}} \frac{\log_2 \det(\boldsymbol{I} + \frac{1}{\sigma^2}\boldsymbol{G}\boldsymbol{\Gamma}\boldsymbol{H}\boldsymbol{Q}\boldsymbol{H}^H\boldsymbol{\Gamma}^H\boldsymbol{G}^H)}{\mu\mathrm{tr}(\boldsymbol{Q}) + P_c} \tag{22a}$$

$$\text{s.t. } \mathrm{tr}(\boldsymbol{\Gamma}\boldsymbol{H}\boldsymbol{Q}\boldsymbol{H}^H\boldsymbol{\Gamma}^H) \le \mathrm{tr}(\boldsymbol{H}\boldsymbol{Q}\boldsymbol{H}^H) \tag{22b}$$

$$\mathrm{tr}(\boldsymbol{Q}) \le P_{max}. \tag{22c}$$

Problem (22) is a fractional maximization program, in which the fractional objective has concave numerator and affine denominator. The constraint equations are also affine. Thus, (22) can be solved by direct use of fractional programming methods [12], e.g., an adaptation of Dinkelbach's algorithm[4]. The performance of such a factional programming algorithm, coupled with an alternating optimization algorithm for Problem (13) whose full description is relegated to the extended version of the work [10] due to space limitation, is later reported for comparison with the codebook-based covariance optimization addressed by Section IV-B.

[4]The modification of standard Dinkelbach's approach takes into account the fact that Problem (22) does not allow the diagonalization of the covariance matrix $\boldsymbol{Q}$, as a direct consequence of the consideration of RHSs with global reflection constraints, which leads to (22c).

B. Optimization by codebook search

The suboptimum (lower-complexity) approach to covariance matrix optimization proposed in this section is based on the use of standard-compliant Type-I and Type-II codebooks. These codebooks define unit-rank covariance matrices based on a discrete Fourier transform construction. Specifically, let us consider a cross-polarization single-panel antenna array with (N_1, N_2) denoting the number of antenna elements along horizontal and vertical axes in a single polarization. Thus, the aggregate count of transmit antenna elements is $2N_1N_2$, accounting for polarization diversity. Introducing the oversampling factors (O_1, O_2) enables the construction of a beam grid based on two-dimensional (2D) DFT principles [13]. Practical implementations typically limit O_i to moderate values (e.g., $O_i \le 4$) to maintain reasonable feedback overhead while still achieving good performance [14]. For $i = 1, 2$, the oversampled DFT beams in one orientation can be formulated as follows:

$$\begin{aligned} &\boldsymbol{\mu}^i(\theta_i) = \left[\begin{array}{cccc} 1 & e^{j\frac{2\pi\theta_i}{N_iO_i}} & \cdots & e^{j\frac{2\pi\theta_i(N_i-1)}{N_iO_i}} \end{array}\right]^T, \\ &\theta_i \in \{0, 1, \ldots, N_iO_i - 1\}, \end{aligned} \tag{23}$$

where θ_i are beam indexes along the horizontal ($i = 1$) and vertical ($i = 2$) directions. Based on the antenna configuration and oversampling ratios specified in [14], a series of 2D DFT spatial domain beams is generated:

$$\mathcal{D} = \left\{\boldsymbol{b}_{\theta_1,\theta_2} \mid \boldsymbol{b}_{\theta_1,\theta_2} = \boldsymbol{\mu}^1(\theta_1) \otimes \boldsymbol{\mu}^2(\theta_2)\right\}, \tag{24}$$

with $\otimes$ denoting the Kronecker product. Here, $\boldsymbol{b}_{\theta_1,\theta_2} \in \mathbb{C}^{N_1N_2\times 1}$ represents an oversampled 2D DFT beam, and $|\mathcal{D}| = N_1O_1 \times N_2O_2$.

Through beam selection and phase tuning, the Type-I codebook $\mathcal{C}_I$ is derived, whereas the Type-II codebook $\mathcal{C}_{II}$ emerges by selecting a subset of beams and adjusting their linear combination coefficients for beam fusion [15], employing identical subsets across polarizations. The Type-II codebook offers superior adaptability by combining multiple beams with optimized weights, effectively creating beam patterns tailored to the channel's dominant directions while maintaining reasonable feedback overhead.

For single-stream transmission, the Type-I codebook vectors are written as:

$$\boldsymbol{w}_{\mathrm{I}}(\theta_1, \theta_2) = \frac{1}{\sqrt{2N_1N_2}}\begin{bmatrix} \boldsymbol{b}_{\theta_1,\theta_2} \\ \varphi\boldsymbol{b}_{\theta_1,\theta_2} \end{bmatrix}, \tag{25}$$

where the scalar $\varphi \in \{1, j, -1, -j\}$ accounts for the phase difference across two polarization directions. The definition of w_{I} relies on the parameters φ, θ_1, and θ_2, leading to a codebook with a total of $4 \times N_1O_1 \times N_2O_2$ possible vectors w_{I}, with the factor 4 accounting for the fact that φ takes values in the set $\{1, j, -1, -j\}$.

For single-stream transmission based on the combination of K beams, the Type-II codebook is represented by:

$$\boldsymbol{w}_{\mathrm{II}}(\boldsymbol{\theta}_1, \boldsymbol{\theta}_2) = \begin{bmatrix} \sum_{k=0}^{K-1} \boldsymbol{b}_{\theta_1^{(k)},\theta_2^{(k)}} p_{1,k}^{\mathrm{WB}} p_{1,k}^{\mathrm{SB}} c_{1,k} \\ \sum_{k=0}^{K-1} \boldsymbol{b}_{\theta_1^{(k)},\theta_2^{(k)}} p_{2,k}^{\mathrm{WB}} p_{2,k}^{\mathrm{SB}} c_{2,k} \end{bmatrix}, \tag{26}$$

where $\boldsymbol{\theta}_1 \triangleq (\theta_1^{(k)})_{k=1}^K$ and $\boldsymbol{\theta}_2 \triangleq (\theta_2^{(k)})_{k=1}^K$. Each element encapsulates a linear blend of K beams from $\mathcal{D}$ for a given polarization. The coefficients $p_{\ell,k}^{\mathrm{WB}}$, $p_{\ell,k}^{\mathrm{SB}}$, and $c_{\ell,k}$ correspond to the wideband amplitude combination, subband amplitude combination, phase combination for polarization ℓ, where $\ell = 1, 2$, and beam k, $\theta_i^{(k)}$ being the kth DFT beam direction indices. The procedure for merging K beams to approximate the wideband channel information as closely as possible involves the use of a wideband beam combining coefficient matrix. The amplitudes of this matrix are normalized according to the strongest beam, which is quantized using a 3-bit scheme to produce $p_{\ell,k}^{\mathrm{WB}}$ [14].

Finally, we can build the transmit covariance matrix by searching in the codebook (either Type-I or Type-II) the optimal beamforming vector. To elaborate, for any beamforming vector in the codebook, we can form the covariance matrix $\boldsymbol{Q}_\ell = a\widetilde{\boldsymbol{Q}}_\ell$, with $\widetilde{\boldsymbol{Q}}_\ell = \boldsymbol{w}_\ell \boldsymbol{w}_\ell^H$, with $\ell = 1$ for Type-I codebooks and $\ell = 2$ for Type-II codebooks. We also notice that the codebook is constructed in order to have $\mathrm{tr}(\boldsymbol{Q}_\ell) = a$, which means that the EE can be rewritten as

$$\mathrm{EE} = \frac{\log_2 \left| \boldsymbol{I} + \frac{a}{\sigma^2} \boldsymbol{G}\boldsymbol{\Gamma}\boldsymbol{H}\widetilde{\boldsymbol{Q}}_\ell \boldsymbol{\Gamma}^H \boldsymbol{G}^H \right|}{\mu a + P_c} , \tag{27}$$

Thus, $\widetilde{\boldsymbol{Q}}_\ell$ and the scalar a can be found by solving

$$\max_{a, \widetilde{\boldsymbol{Q}}_\ell} \frac{\log_2 \left| \boldsymbol{I} + \frac{a}{\sigma^2} \boldsymbol{G}\boldsymbol{\Gamma}\boldsymbol{H}\widetilde{\boldsymbol{Q}}_\ell \boldsymbol{\Gamma}^H \boldsymbol{G}^H \right|}{\mu a + P_c} \tag{28a}$$

$$\text{s.t. } \mathrm{tr}(\boldsymbol{\Gamma}\boldsymbol{H}\widetilde{\boldsymbol{Q}}_\ell \boldsymbol{H}^H \boldsymbol{\Gamma}^H) \leq \mathrm{tr}(\boldsymbol{H}\widetilde{\boldsymbol{Q}}_\ell \boldsymbol{H}^H) \tag{28b}$$

$$a \leq P_{max}. \tag{28c}$$

Problem (28) can be solved by searching for $\widetilde{\boldsymbol{Q}}_\ell$ in the codebook (either Type-I or Type-II) with cardinality $N_1 N_2 O_1 O_2 = N_T O_1 O_2 / 2$. For each candidate matrix $\widetilde{\boldsymbol{Q}}_\ell$ the scalar a can be determined by solving a simple scalar problem. The resulting alternating optimization method based on codebook search is summarized in Algorithm 2.

Algorithm 2 EE maximization by codebook search

```
Choose ε > 0;
Set (Q_0, Γ_0) to feasible values;
repeat
  Let Γ be the output of Algorithm 1, given Q_0;
  Let Q be the solution of (28), given Γ;
  Err = |EE(Γ, Q) − EE(Γ_0, Q_0)|;
  Q_0 = Q; Γ_0 = Γ;
until Err ≤ ε
```

Remark 1. *Algorithm 2 can be specialized to perform capacity maximization instead of EE maximization by simply setting* $\mu = 0$ *in* (28a).

Remark 2. *Since the codebook cardinality is* $N_T O_1 O_2 / 2$*, the complexity of Algorithm 2 can be evaluated as*

$$\mathcal{C}_{CB} = \mathcal{O}\left(I_{alt,CB} \left(I_{seq,CB} N^4 + N_T O_1 O_2 \right) \right) . \tag{29}$$

Here, $I_{alt,CB}$ *and* $I_{seq,CB}$ *are the number of iterations until convergence of the Algorithm 2 and of the sequential algorithm that is run inside Algorithm 2. Moreover, the complexity of the codebook search can be tuned by choosing* O_1 *and* O_2 *in order to have a finer or coarser resolution of the codebook.*

V. Numerical Results

For our numerical analysis, we have considered a base station with $N_T = 4$ antennas that communicates with a single-antenna user equipment placed at a distance of 100 m. The BS is placed at a height of 10 m from the ground, while the user equipment is placed at a height of 1.5 m. The carrier frequency is 3.5 GHz, the communication bandwidth is 20 MHz, the thermal noise power spectral density is -174 dBm/Hz, the noise figure at the receiver is 5 dB. The RHS has N reflecting elements, each consuming a power of $P_{c,n} = 0$ dBm. The rest of the system static power consumption is $N_T P_{c,t} + N_R P_{c,r} + P_{c,0} = 57$ dBm.

Fig. 1 shows the capacity versus the number N of RHS reflecting elements, achieved, for $P_{max} = 40$ dBm, by the following schemes:

- Optimization of $\boldsymbol{Q}$ and $\boldsymbol{\Gamma}$ for capacity maximization by the Dinkelbach's Algorithm (labeled Opt. $\boldsymbol{Q}$ - Opt. RHS).
- Optimization of $\boldsymbol{Q}$ and $\boldsymbol{\Gamma}$ for capacity maximization by the proposed Algorithm 2.
- Optimization of $\boldsymbol{Q}$ for capacity maximization by Dinkelbach's algorithm and random $\boldsymbol{\Gamma}$ (labeled Opt. $\boldsymbol{Q}$ - Random RHS).
- Optimization of $\boldsymbol{Q}$ for capacity maximization by codebook search and random $\boldsymbol{\Gamma}$.
- Optimization of $\boldsymbol{\Gamma}$ for capacity maximization and uniform and independent power allocation among the transmit antennas.
- Random $\boldsymbol{\Gamma}$ and uniform and independent power allocation among the transmit antennas.

As expected, the capacity increases with the number of reflecting elements, and the best results are provided by reference Dinkelbach's Algorithm. Nevertheless, Algorithm 2 entails a limited performance degradation compared to the the former one. Moreover, it is shown that both algorithms increase the capacity with respect to simpler schemes that do not perform any optimization, or that optimize only either the RHS or $\boldsymbol{Q}$.

Finally, Fig. 2 shows the EE versus the number N of RHS reflecting elements, achieved, for fixed $P_{max} = 40$ dBm, by the same resource allocation schemes of Fig. 1. Similar observations to those for Fig. 1 can be made, with the notable difference that the EE obtained with uniform power allocation (i.e. no optimization of $\boldsymbol{Q}$) and RHS optimization is significantly worse than the corresponding capacity that is shown in Fig. 1. This is explained because the uniform power allocation is a strategy that employs all the available power P_{max}, and in Fig. 2 it was set $P_{max} = 40$ dBm, which is a rather high power value. Thus, adopting uniform power allocation with $P_{max} = 40$ dBm is entails a greater degradation of the EE, as shown in Fig. 2, than the capacity (shown in Fig. 1). Moreover, it can be noticed that the EE increases with N at a lower rate than the capacity. This is

due to the fact that, as N increases, both the capacity and the hardware power consumption increase. Eventually, for larger values of N, the EE decreases with N since the numerator increases only logarithmically while the denominator increases linearly with N.

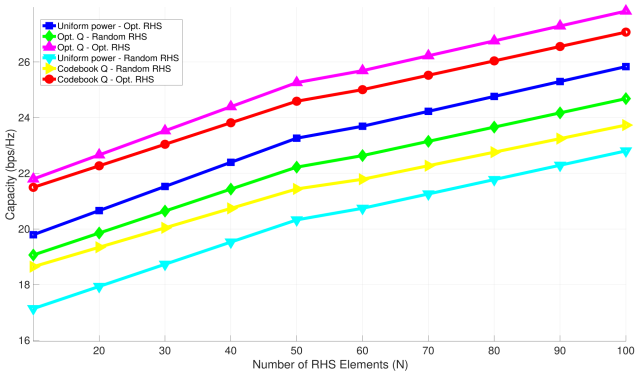

Fig. 1. Capacity versus number of reflecting elements of the RHS for different resource allocation policies.

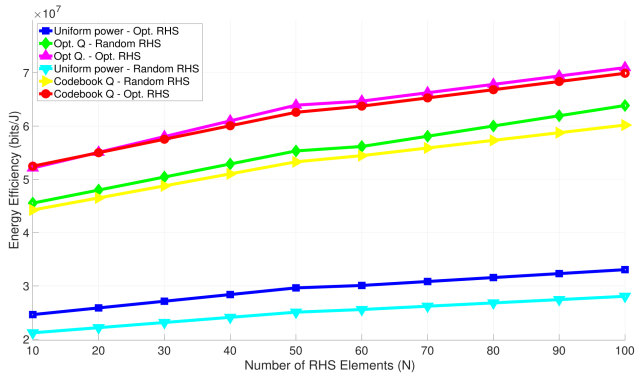

Fig. 2. EE versus number of reflecting elements of the RHS for different resource allocation policies.

VI. Conclusion

In this work, we considered a wireless MIMO link where data transmission was supported by an RHS placed in the near field of the transmit antenna array. The objective was to optimize both the system's EE and capacity by jointly allocating the transmit covariance matrix and the RHS reflection matrix. To optimize the RHS, we employed a sequential optimization approach, which allowed for the efficient tuning of the reflection matrix. For the optimal transmit covariance matrix, we explored two approaches: one based on sequential fractional programming and another involving a search within a standard-compliant codebook. These two algorithms offered distinct trade-offs in terms of performance and complexity. The codebook-based method, while simpler and computationally less demanding, incurred a small performance penalty. In contrast, the fractional programming approach, although more complex and requiring greater computational resources, provided higher performance. This comparison highlights the balance between computational efficiency and performance optimization in the system design.

Acknowledgments

The work of A.I. Tunali was funded by the European Commission through the project HE-DN-INTEGRATE, grant agreement number 101072924. The work of R. Fotock was funded by the Project "GARDEN" within the NextGeneration EU plan, Mission 4, Component 1, CUP H53D23000480001, through the Italian "Bando Prin 2022 - D.D. 104 del 02-02-2022" by MUR. The work of A. Zappone was funded by the European Union - NextGenerationEU under the project NRRP RESTART, RESearch and innovation on future Telecommunications systems and networks, to make Italy more smART PE_00000001 - Cascade Call SPARKS project, with CUP D43C22003080001.

References

[1] Huawei Technologies, "Green 5G building a sustainable world," *https://www.huawei.com/en/public-policy/green-5g-building-a-sustainable-world*, 2020.

[2] R. Long, Y. C. Liang, Y. Pei, and E. G. Larsson, "Active reconfigurable intelligent surface-aided wireless communications," *IEEE Transactions Wireless Communications*, vol. 20, no. 8, pp. 4962–4975, Aug. 2021.

[3] R. K. Fotock, A. Zappone, and M. Di Renzo, "Energy efficiency optimization in RIS-aided wireless networks: Active versus nearly-passive RIS with global reflection constraints," *IEEE Transactions on Communications*, vol. 72, no. 1, pp. 257–272, 2023.

[4] A. Zappone, M. Di Renzo, F. Shams, X. Qian, and M. Debbah, "Overhead-aware design of reconfigurable intelligent surfaces in smart radio environments," *IEEE Transactions on Wireless Communications*, vol. 20, no. 1, pp. 126–141, 2021.

[5] L. You, J. Xiong, D. W. K. Ng, C. Yuen, W. Wnag, and X. Gao, "Energy efficiency and spectral efficiency tradeoff in RIS-aided multiuser MIMO uplink transmission," *IEEE Transactions on Signal Processing*, pp. 1407–1421, 2021.

[6] V. Sharma *et al.*, "A pricing-based approach for energy-efficiency maximization in RIS-aided multi-user MIMO SWIPT-enabled wireless networks," *IEEE Access*, vol. 10, pp. 29 132–29 148, 2022.

[7] M. Soleymani, I. Santamaria, E. A. Jorswieck, R. Schober, and L. Hanzo, "Optimization of the downlink spectral- and energy-efficiency of RIS-aided multi-user URLLC MIMO systems," *IEEE Transactions on Communications*, 2024.

[8] V. Degli-Esposti, E. M. Vitucci, M. Di Renzo, and S. Tretyakov, "eradiation and scattering from a reconfigurable intelligent surface: A general macroscopic mode," *IEEE Transactions on Antenna and Propagation*, vol. 70, no. 10, pp. 8691—8706, 2022.

[9] C. Feng, H. Lu, Y. Zeng, T. Li, S. Jin, and R. Zhang, "Near-field modelling and performance analysis for extremely large-scale IRS communications," *IEEE Transactions on Wireless Communications*, vol. 23, no. 5, pp. 4976–4989, 2024.

[10] A. I. Tunali, R. K. Fotock, A. Zappone, G. Taricco, G. Alfano, and H. A. Çirpan, "Energy efficiency maximization in mimo links aided by metasurfaces with global reflection constraints," 2025, *submitted to EURASIP Journal on Advances in Signal Processing*.

[11] B. R. Marks and G. P. Wright, "A general inner approximation algorithm for non-convex mathematical programs," *Operations Research*, vol. 26, no. 4, pp. 681–683, 1978.

[12] A. Zappone and E. A. Jorswieck, "Energy efficiency in wireless networks via fractional programming theory," *Found. and Trends® in Commun. and Inf. Theory*, vol. 11, no. 3-4, pp. 185–396, 2015.

[13] Ericsson, "Advanced CSI codebook structure," Ericsson, TSG-RAN WG1 #87 RI-161266, 2016.

[14] 3GPP, "NR; Physical layer procedures for data," 3rd Generation Partnership Project (3GPP), Technical Specification (TS) 38.214, 01 2024, version 18.1.0. [Online]. Available: https://portal.3gpp.org/desktopmodules/Specifications

[15] Intel, "On NR Type I codebook," Intel, TSG RAN WG1 #88 R1-1702205, 2017.